

# Comparative Study of Wind Loads on Tall Buildings of Different Shapes



Rahul Kumar Meena , Ritu Raj , and S. Anbukumar 

## Nomenclature

$A$	Frontal area of rotor ( $\text{m}^2$ )
AR	Aspect ratio
$C_p$	Pressure coefficient
$\theta$	Angle of attack of wind ( $^\circ$ )
$\rho$	Density of air ( $\text{kg}/\text{m}^3$ )
$\Omega$	Omega
$\varepsilon$	Epsilon
$\alpha$	Roughness coefficient 0.147

## 1 Introduction

With the advancement of technology and enormous population growth, the need and design of high structures with different configurations have been a growing trend. High-rise structures have always fascinated from the beginning of civilization and are unique in various aspects, such as consideration of lateral deflections. The wind is a complicated phenomenon in which the motion of an individual particle is so unpredictable that one needs to be concerned about the statistical distribution of velocity rather than just simple averages. There are two distinct local influences in determining overall wind power, even if windward pressure and leeward suction add up to one total. When it comes to wind load planning, a structure cannot be considered to have a

---

R. K. Meena (✉) · R. Raj · S. Anbukumar  
Delhi Technological University, Delhi 110042, India  
e-mail: [rahul.08dtu@gmail.com](mailto:rahul.08dtu@gmail.com); [rahulkumar\\_phd2k18@dtu.ac.in](mailto:rahulkumar_phd2k18@dtu.ac.in)

regular configuration by default. Designers use wind load standards to compute structural pressure coefficients and force coefficients for other structures that are exposed to wind-induced stresses [1–5]. On the other hand, these standards offer details for plain cross-sectional configurations with a limited number of wind incidence angles. These codes do not provide information on wind loadings for structures with different configurations. As a result, wind tunnel research on models of such forms is popular. Chandan and Kumar [6] simulating wind studies of towering structures was accomplished with the use of CFD (computational fluid dynamics). CFD can yield results that are comparable to those obtained from wind tunnel studies. CFD might examine the entire domain study, provide better visualization of data and be less expensive than wind tunnel tests. Raj and Ahuja [7] The use of a boundary layer wind tunnel was used to conduct experimental study on the wind load on high structures with cross-plan configurations. Bairagi and Dalui [8] as a result of increased turbulence, positive pressure built up in the setback roof, where turbulence is at its most severe, and the largest spectral density frequency was formed at this place. Using CFD simulations for wind incidence angles ranging from  $0^0$  to  $180^0$ , this article examined the influence of aerodynamics on the setback of tall structures. Hajra and Dalui [9] performed the mathematical-based research of interference effect on octagonal plan configuration high structure using CFX (ANSYS), for  $0^0$  wind incidence angle using  $k - \varepsilon$ , SST and  $k - \omega$  model, and analysis of these three models shows nearly identical results. Meena et al. [10] research has been carried out to determine how wind affects different types of multi-storey steel structures' bracing mechanisms. Verma et al. [11] for the  $0^0$ ,  $15^0$  and  $30^0$  wind speeds, the influence of wind load on a high octagonal configuration structure was investigated using computational fluid dynamics (CFD) simulation. This demonstrated that CFD may be utilized to forecast wind-related problems on tall structures with complicated geometries. The conclusions of wind-induced response are dependent on the type of plan in geometry and defining the flow properties. Dalui et al. [12] studied the effects of interference on octagonal plan configuration high structures under the influence effect of wind, windward face and immediate side face to windward face is not affected much by the presence of the interfering structure. Paterka et al. [13] discussed the wind flow pattern around the structures. Wind flow about three-dimensional structures results in separated flow regions fundamentally highly different from those about two-dimensional structures. In three-dimensional, as opposed to two-dimensional modelling, the separation of cavities immediately downwind is not encased by free streamlines. Kawamoto [14] for the assessment of wind load on the structure, a cost-effective turbulence model was created. The mean pressure coefficient improves considerably when employing the  $k - \omega$  turbulence model, and the over prediction of turbulence kinetic energy in the  $k$ -turbulence model is the source of the error in the  $k - \varepsilon$  turbulence model. Pal et al. [15] looked at both square and fish floor layouts. It is the most efficient design in terms of wind-generated pressure and base shear when completely blocked, compared to other designs. Amin and Ahuja [16] suction on side faces and leeward faces is greatly affected by the plan arrangement of the model and wind incidence angle, according to experimental studies of wind-induced pressure on structures of various geometries. Selvem [17] by employing large eddy

simulation, the Navier–Stokes equation was numerically solved, resulting in a peak pressure that is substantially greater than that measured in the field. As compared to the three turbulence models, the peak pressure calculated using TTU wind data is substantially closer to the measurements taken in the field. Pirooz and Flay [18] the impacts of a solid tower and an urban environment on collected wind data were explored, as well as numerical and wind tunnel simulations. Some researchers have also explained few important characteristics of wind using wind tunnel test like pal et al. [19] on isolated fish plan shape building, Nagar et al. [20] on plus plan shape building, Pal et al. [21] interference study on same-type building, Kumar and Raj [22] on oval shape building, Gaur and Raj [23] on plus shape, Meena et al. [24] on “L” shape, Mahajan et al. [25] on the effect of shear wall on different corner shape structure, Gaur et al. [26] interference study on wind effects and Nagar et al. [27] on different shape of high-rise structure. In this study, the influence of shape of high-rise structure is obtained using the numerical simulation performed using ANSYS CFX on hexagon and octagon shape building model. The entire numerical simulation is performed by utilizing the  $k - \epsilon$  turbulence model. The domain is considered such that no recirculation of flow can occur.

## 2 Numerical Modelling

The present study is carried out to obtain pressure contour and pressure coefficient for a different types of high structure using the ANSYS CFX package (Version 2020 R-2).

### 2.1 Model and Boundary Conditions

The purpose of this research is to determine the wind effects on hexagon model A (a) and octagon model B (b) at a  $0^\circ$  wind incidence angle. Figure 1 shows the dimensions of the structure as well as the angle of wind incidence.

As shown in Fig. 2, domain is where all the solution of CFD simulation is done and is provided according to Revuz [28]. Domain side wall, inlet and top wall are kept at 5H. The outlet is kept at 15H, where  $H$  is the height of the structure.

Domain top wall and side wall are kept as free slip wall, and model face and ground are kept as no-slip wall.

### 2.2 Meshing

Meshing is provided to increase the accuracy of the solution done during simulation. This can be provided by manual and automatic using ANSYS CFX. In the manual

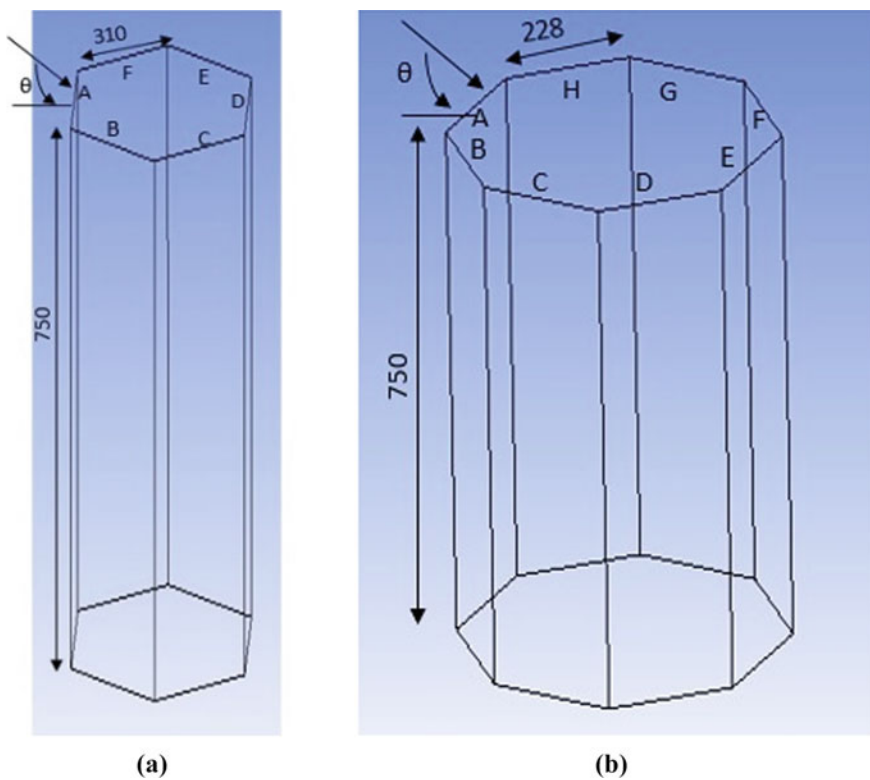


**Fig. 1** Model dimension, face name and wind incidence angle **a** model A, **b** model B

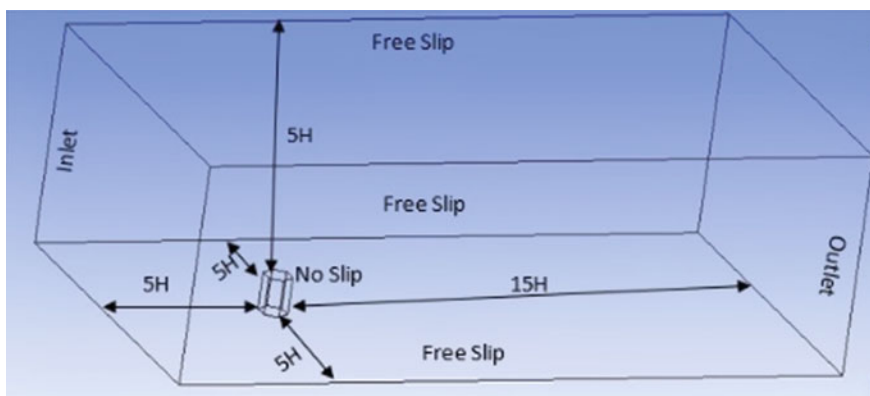


**Fig. 2** Domain

method, meshing for different parts can be applied, and depending on the problem, meshing size is selected. The inflation done in CFD simulation for all models is used to reduce the anomalous flow. As shown in Fig. 3, domain provided with tetrahedron meshing, structure and ground meshing is relatively more delicate in size. It increases the solution accuracy. Figure 4a is edge meshing, and Fig. 4b is inflation, used to minimize the unusual flow.

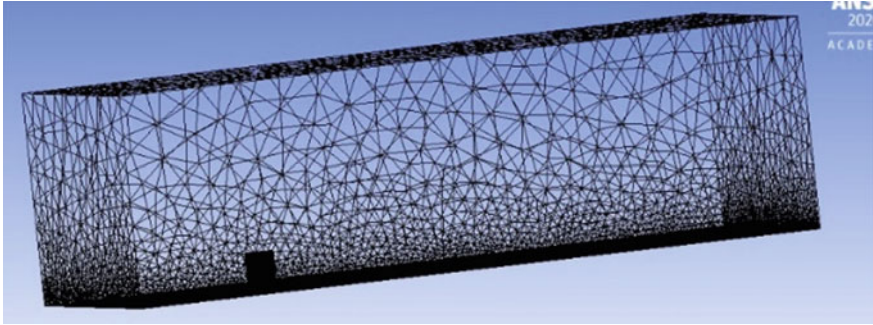


**Fig. 3** Domain, ground and structure meshing

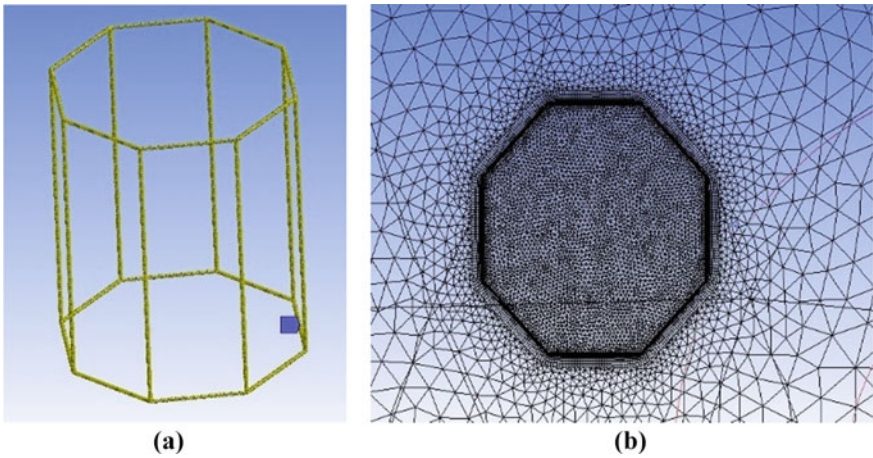


**Fig. 4** Meshing **a** edge meshing **b** inflation

### 3 Result and Discussion

#### 3.1 The Profile of Velocity and Turbulence Intensity

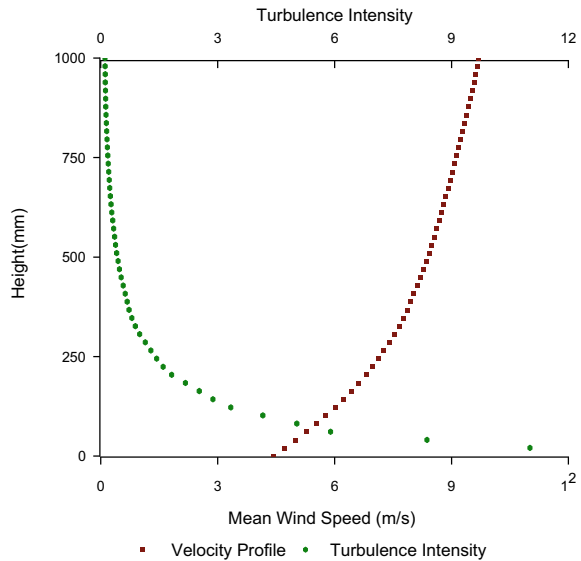
When estimating the vertical profile of wind speed, surface roughness and drag induced by local projections that impede wind flow are important elements. Neither the gradient height nor the gradient velocity causes any drag; these two numbers are referred to as the gradient. The atmospheric boundary layer refers to the layer of air above which topography has an effect on wind speed.

The wind speed profile within the atmospheric boundary layer, as seen in Fig. 5, is determined by equation according to Power Law Eq. (1).

$$\frac{U}{U_H} = \left( \frac{Z}{Z_H} \right)^\alpha \tag{1}$$

where  $U_H$  is the speed at the reference height  $Z_H$ , which is 10 m/s,  $\alpha$  is the ground roughness, that varied as per the terrain conditions, and actual situation in this study is 0.147 for terrain category 2, while  $Z_H$  is 1.0 m for terrain category 2.

**Fig. 5** Height-dependent variations in wind speed and turbulence intensity



### 3.2 Pressure Contours

Figures 6 and 7 show that the pressure applied to the windward face is positive for the models and that it is negative for the windward and leeward faces. As seen by a bar chart in Figs. 6 and 7, models A and B are subjected to varying levels of pressure.

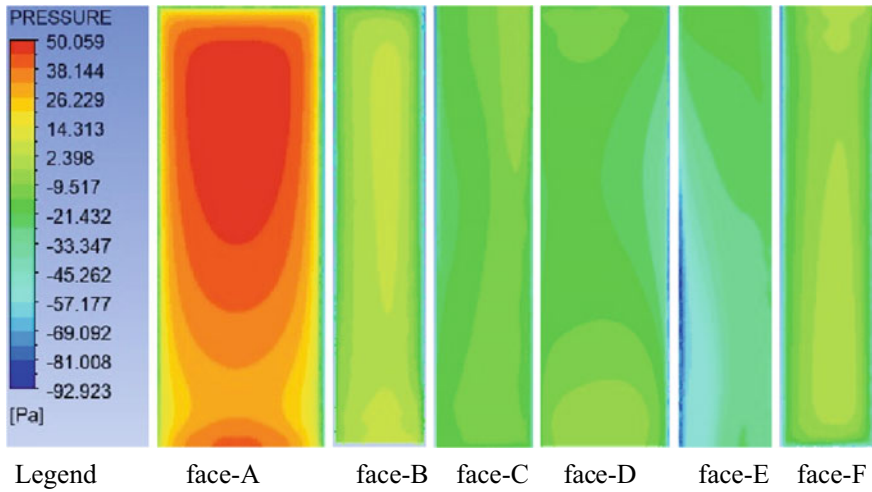


Fig. 6 Pressure contour for model A at 0° wind incidence angle

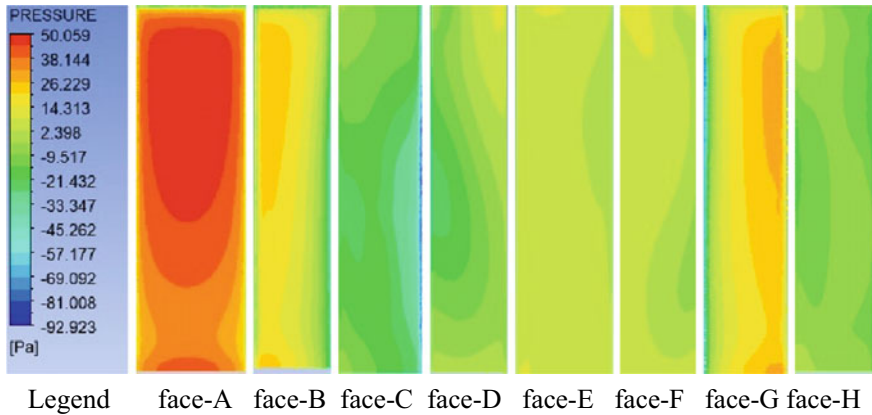


Fig. 7 Pressure contour for model B at 0° wind incidence angle

### 3.3 Velocity Streamlines

At each location along the imaginary line, the direction of a fluid particle's velocity is indicated by the tangent. While moving through the air, a fluid particle is called to be on a streamline. For a wind incidence angle of  $0^0$  degrees, the streamline is symmetric. The model shows how the streamlining will look. Figure 8 shows a structure (a) in plan, (c) in elevation and (e) in three-dimensional view of streamlines at a  $0^0$  wind incidence angle. With a  $0^0$  wind incidence angle, Fig. 8 shows the streamlines for the model B structure (b) in plan, (d) in elevation and (f) in 3D perspective.

The mean  $C_p$  for model B is shown in Fig. 7. It can be seen in Fig. 7 that face A is the only face of model B that is subjected to positive pressure, while the remaining faces of model B are subjected to negative pressure. The  $k - \epsilon$ , SST and  $k - \omega$  models all produce  $C_p$  values that are almost equal for each face.

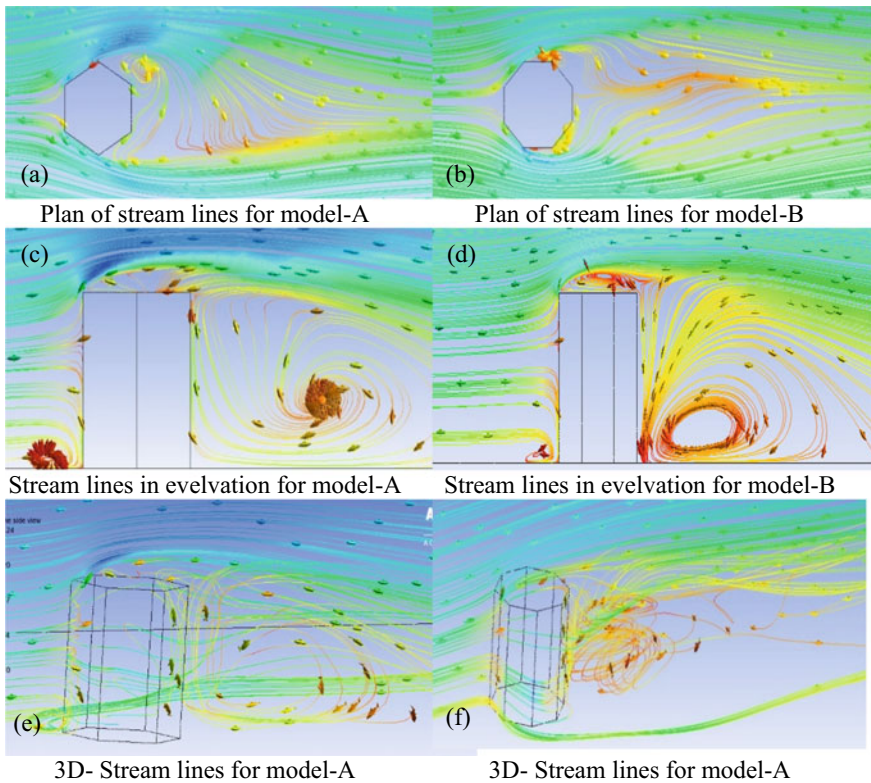


Fig. 8 Streamlines on model A and B



### 3.4 Vertical Centre Line Pressure Coefficient

In both Figs. 9 and 10, the structural height and the mean surface pressure coefficient are shown. Because face A is a windward face, the wind hits it directly as shown in Figs. 9 and 10. Pressure variation due to 0° wind incidence angle is for both the structure models A and B and is shown in Figs. 9 and 10, respectively, around the centreline of every face.

**Fig. 9** Variation in pressure along the centreline for all of the faces of model A

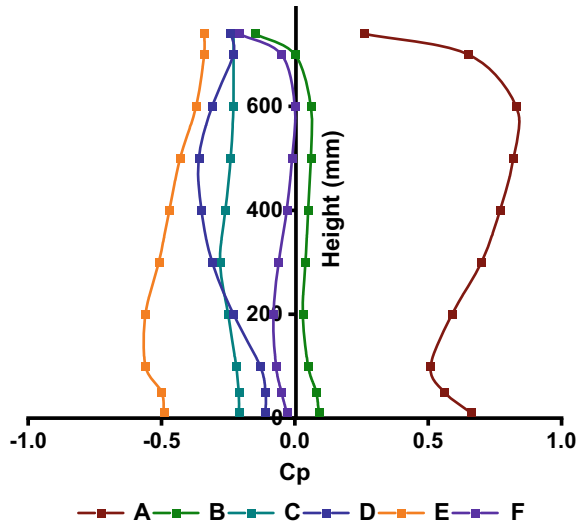
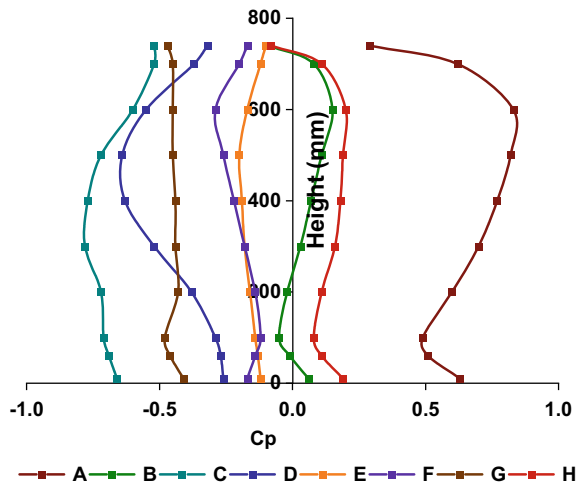


**Fig. 10** Variation in pressure along the centreline for all of the faces of model B



## 4 Conclusion

“Hexagon” and “Octagon” design values of the pressure contours, mean pressure coefficients and velocity streamlines are all examined at  $0^0$  wind incidence angles in this study”.  $K - \varepsilon$  modelling is utilized to replicate this study. The following are the findings of the study:

- Negative pressure is always applied to face *B*, while positive pressure is always applied to face *A* in both models.
- Octagonal tall structure experiences almost symmetrical pressure distribution.
- The fluctuation of pressure coefficients along the centreline is examined and graphically depicted.
- The octagonal and hexagonal plan cross-sectional shape has more or less the same nature of pressure distribution on the windward surface in the case of symmetrical wind incidence angle.
- The velocity streamlines are depicted in the plan, elevation and 3D views using the figure.
- In the same way that a boundary layer wind tunnel determines the precision of the task, meshing the geometry model and setting the flow physics determine the precision of the task.
- This investigation of the wind pressure distribution on the leeward face illustrates the formation of vorticity, which indicates a significant amount of turbulence, according to the findings.

**Acknowledgements** The authors are thankful to Delhi Technological University for providing the research facilities and funding to support this study. The authors are grateful to Asha, Aparna and Rhythem; they encouraged and supported the author throughout this study.

## References

1. IS: 875 (2015) Indian standard design loads (other than earthquake) for buildings and structures—code of practice, part 3(wind loads)
2. ASCE: 7-10 (2013) Minimum design loads for buildings and other structures. Struct Eng Instit Am Soc Civil Eng Reston
3. GB 50009–2001 (2002) National standard of the People’s Republic of China
4. Ethiopian Standard, ES ISO 4354 (2012) (English) Wind actions on structures 2012
5. AS/NZS: 1170.2 (2011) Structural design actions—part 2: wind actions. Standards Australia/Standards New Zealand, Sydney
6. Hima Chandan D, Pradeep Kumar R (2014) Numerical simulation of wind analysis of tall buildings computational fluid dynamics approach
7. Raj R, Ahuja AK (2013) Wind loads on cross shape tall buildings. J Acad Indus Res (JAIR) 2(2):111–113
8. Bairagi K, Dalui SK (2018) Aerodynamic effects on setback tall building using CFD simulation. Int J Mech Prod Eng Res Dev 413–420. (Online). Available: [www.tjprc.org](http://www.tjprc.org)

9. Hajra S, Dalui SK (2016) Numerical investigation of interference effect on octagonal plan shaped tall buildings. *Jordan J Civil Eng* 10(4):462–479
10. Meena RK, Awadhiya GP, Paswan AP, Jayant HK (2018) Effects of bracing system on multistoreyed steel building. <https://doi.org/10.1088/1757-899X/1128/1/012017>
11. Verma DSK, Roy A, Lather S, Sood M (2015) CFD Simulation for wind load on octagonal tall buildings. *Int J Eng Trends Technol* 24(4):211–216. <https://doi.org/10.14445/22315381/ijett-v24p239>
12. Dalui SK, Kar R, Hajra S (2015) Interference effects on octagonal plan shaped tall building under wind—a case study 9:74–81
13. Peterka JA, Meroney RN, Kothari KM (1985) Wind flow patterns about buildings 21:21–38
14. Kawamoto S (1997) Improved turbulence models for estimation of wind loading. *J Wind Eng Ind Aerodyn* 67–68:589–599. [https://doi.org/10.1016/S0167-6105\(97\)00102-5](https://doi.org/10.1016/S0167-6105(97)00102-5)
15. Pal S, Raj R, Anbukumar S (2021) Comparative study of wind induced mutual interference effects on square and fish-plan shape tall buildings. *Sādhanā* 0123456789. <https://doi.org/10.1007/s12046-021-01592-6>
16. Amin J, Ahuja A (2011) Experimental study of wind-induced pressures on buildings of various geometries. *Int J Eng Sci Technol* 3(5):1–19. <https://doi.org/10.4314/ijest.v3i5.68562>
17. Selvam RP (1997) Computation of pressures on Texas Tech University building using large eddy simulation. *J Wind Eng Ind Aerodyn* 67–68:647–657. [https://doi.org/10.1016/s0167-6105\(97\)00107-4](https://doi.org/10.1016/s0167-6105(97)00107-4)
18. Safaei A, Flay RGJ (2019) Effects of a solid tower and urban area on measured wind data : numerical and wind-tunnel simulations: 6–9
19. Pal S, Meena RK, Raj R, Anbukumar S (2021) Wind tunnel study of a fish—plan shape model under different isolated wind incidences 5:353–366
20. Nagar SK, Raj R, Dev N (2021) Proximity effects between two plus-plan shaped high-rise buildings on mean and RMS pressure coefficients. *Sci Iran* 0–0. <https://doi.org/10.24200/sci.2021.55928.4484>
21. Pal S, Raj R, Anbukumar S (2021) Bilateral interference of wind loads induced on duplicate building models of various shapes. *Latin Am J Solids Struct* 18(5). <https://doi.org/10.1590/1679-78256595>
22. Kumar A, Raj R (2021) Study of pressure distribution on an irregular octagonal plan oval-shape building using CFD. *Civil Eng J* 7(10):1787–1805. <https://doi.org/10.28991/cej-2021-03091760>
23. Gaur N, Raj R (2021) Aerodynamic mitigation by corner modification on square model under wind loads employing CFD and wind tunnel. *Ain Shams Eng J*. <https://doi.org/10.1016/j.asej.2021.06.007>
24. Meena RK, Raj R, Anbukumar S (2021) Numerical investigation of wind load on side ratio of high-rise buildings numerical investigation of wind load on side ratio of high-rise buildings. Springer, Singapore
25. Mahajan S, Yadav V, Raj R, Raj R (2022) Effect of shear walls on tall buildings with different corner configuration subjected to wind loads. In: Gupta AK, Shukla SK, Azamathulla H (eds) *Advances in Construction Materials and Sustainable Environment. Lecture Notes in Civil Engineering*, vol 196. Springer, Singapore. [https://doi.org/10.1007/978-981-16-6557-8\\_59](https://doi.org/10.1007/978-981-16-6557-8_59)
26. Gaur N, Raj R, Goyal PK (2021) Interference effect on corner—configured structures with variable geometry and blockage configurations under wind loads using CFD. *Asian J Civil Eng*. <https://doi.org/10.1007/s42107-021-00400-0>
27. Nagar SK, Raj R, Dev N (2020) Experimental study of wind-induced pressures on tall buildings of different shapes. *Wind Struct Int J* 31(5):441–453. <https://doi.org/10.12989/was.2020.31.5.431>
28. Revuz J, Hargreaves DM, Owen JS (2012) On the domain size for the steady-state CFD modelling of a tall building. *Wind Struct Int J* 15(4):313–329. <https://doi.org/10.12989/was.2012.15.4.313>